Approaches to the design of the new high-strength casting aluminum alloys of 7xxx series with high iron content

UDC 669.71.055

T. K. Akopyan, *Researcher of Engineering Center "Casting Technologies and Materials"*[1,2], *e-mail: nemiroffandtor@yandex.ru*
N. A. Belov, *Professor of a Chair Casting Technologies and art metal processing*[1]

[1] *National University of Science and Technology "MISIS", Moscow, Russia.*
[2] *Baikov Institute of Metallurgy and Materials Science, Russian Academy of Sciences, Moscow, Russia.*

The most high-strength aluminum alloys based on the Al – Zn – Mg – (Cu) system have a significant tendency to form hot cracks during solidification. Additional alloying of 7xxx series alloys with the eutectic forming elements (Fe and Ni) that are slightly soluble in an (Al) solid solution was proposed in order to reduce the hot cracking tendency. In this case, the iron becomes an alloying element, rather than an harmful impurity. Since the appearance of primary crystals of the iron- and nickel-bearing phases is unacceptable, the boundaries of primary crystallization of (Al), Al_9FeNi, Al_3Ni and Al_3Fe phases (the liquidus projection) were computed using Thermo-Calc software. In accordance with the results of thermodynamic calculations of the multicomponent Al – Zn – Mg – Cu – Fe – Ni phase diagram, the new sparingly alloyed alloy ATs6N0.5Zh (Al – 6.3% Zn – 2.1% Mg – 0.2% Cu – 0.4% Fe – 0.6% Ni) based on the (Al) + Al_9FeNi eutectic was selected. The results of the fracture surface analysis of the castings after ageing show the mode of fracture is the dimple rupture. Traces of intergrain fracture typical for high-alloyed alloys of the 7xxx series without eutectic inclusions are not observed. Defect-free experimental samples with high mechanical properties (σ_r ~ 500 MPa, $\sigma_{0.2}$ ~ 450 MPa, δ ~ 4.7%) using liquid forging were obtained from the ATs6N0.5Zh alloy.

Key words: high-strength aluminum alloys, phase composition, phase diagrams, thermodynamic calculations, castings, mechanical properties.

DOI: *http://dx.doi.org/10.17580/nfm.2016.01.04*

Introduction

High-strength aluminum alloys take a special place because they are used in critical parts, in particular, in aviation and rocket building. Alloys based on the Al – Zn – Mg – Cu system possess the highest strength properties among commercial aluminum alloys [1–9], however, these alloys have a number of disadvantages. In the first place, the high tendency to hot cracking during solidification does not allow to use these alloys as casting. Moreover, the traditional high-strength aluminum alloys should have low content of iron and silicon, i. e., its production requires high-purity aluminum and this narrows the range of its applications [10].

Additional alloying of the high-strength alloys with the eutectic forming elements that are slightly soluble in an (Al) solid solution was proposed in order to reduce the hot cracking tendency. Alloying with these elements leads to the narrowing of the solidification range by the formation of two- and three-phase eutectics; the required level of the mechanical properties is ensured by the composition of aluminum matrix.

In terms of this concept, two new high-strength aluminum alloys (which were called nikalins — ATs6N4 and ATs7Mg3N4) based on the (Al) + Al_3Ni eutectic and containing (Σ(Zn + Mg) ~10% (wt.)) were developed at MISiS, Moscow [11–14]. These alloys have proved to have a very high strength in castings (σ_r more than 550 MPa, δ = 5–6%) and enough good casting properties. However, they should be considered as model compositions, since the iron content in them is low due to a high content (up to 4%) of expensive nickel; i. e., the production of these alloys requires high-purity aluminum. This fact excludes a wide application of these alloys.

We have suggested an alternative approach to creating alloys with a high content of zinc and magnesium using an (Al) + Al_9FeNi eutectic as a base. This eutectic possesses characteristics close to those of (Al) + Al_3Ni [15, 16] but is more expedient due to the lower content of nickel. In that case the iron becomes an alloying component rather than a harmful impurity.

The aim of the present study is to optimize phase composition optimization of the new aluminum alloys group, i. e., sparingly alloyed high-strength nikalins based

on the (Al) + Al_9FeNi eutectic using both thermodynamic calculations and experimental investigations. These alloys contain at least 0.5% (wt.) of Fe and exhibit enhanced castability.

Experimental section

The object of experimental inquiry was ATs6N0.5Zh alloy, which was prepared using aluminum A7 (99.97% purity), zinc Ts0 (99.9% purity), magnesium Mg90 (99.9% purity), and Al – 10% Fe and Al – 20% Ni master alloys. The alloy was melted using a laboratory resistance furnace and graphite-chamotte crucibles. Rectangular ingots of 15 mm thick, 30 mm wide, and 200 mm long were prepared by casting into a graphite mold. The chemical composition of the experimental alloy is given in Table 1 in accordance with spectral analysis data, which was performed with an ARL 4460 spectrometer.

Thermodynamic calculations including the construction of isothermal and polythermal sections and the determination of the solidus (*ts*) and solvus (*tss*) temperatures, the chemical compositions, and the volume fractions (Q_V) of the solid phases fracture depending on the temperature in the interval of the non-equilibrium and equilibrium solidifications were performed using the Thermo-Calc software (TCW5 version, TTAL5 data base).

The microstructure of cast and heat treated samples was studied using a JSM-6610LV scanning electron microscope (SEM). The JSM-6610LV SEM is equipped with an INCA SDD X-MAX energy dispersive microanalyzer (Oxford Instruments) and the INCA Energy software, which allow one to perform electron-probe microanalysis (EPMA) and to obtain composition profiles and element distribution maps. The sections cut from the central area of cast and heat-treated ingots were studied. The sections were prepared by both mechanical and electrolytic polishing using an electrolyte that consists of C_2H_5OH, $HClO_4$, and glycerol taken in the ratio 6:1:1. Electrolytic polishing was performed at a voltage of 12 V.

The mechanical properties of the castings (the ultimate tensile strength σ_r and the elongation δ) were determined from the results of the tests for uniaxial tension using a Zwick Z250 universal testing machine at room temperature. The three samples were tested under each processing condition. The testing speed was 10 mm/min.

A cooling curve of ATs6N0.5Zh alloy were obtained by laboratory stand. The principle of operation of the stand is based on measuring of the alloy temperature using the chromel-alumel thermocouples. The crucible with a metal was placed in a furnace and heated to 730 °C, and then get out and cooled in air to 300 °C.

Table1.

Chemical compositions of model aluminum alloys

Content of elements, % (wt.)				
Zn	Mg	Cu	Ni	Fe
6.29	2.11	0.16	0.62	0.41

Results and discussion

To solve the hot cracking problem of the Al – Zn – Mg – Cu-based aluminum alloys, the idea of additionally alloying them with low solubility elements in (Al) was proposed. Alloying with these elements leads to narrowing the solidification range by the formation of two- and three-phase eutectics and the required level of the mechanical properties is ensured by the composition of aluminum matrix. In general, the new aluminum eutectic type alloys should satisfy the following conditions:

– the eutectic phase quantity should be large enough to ensure high castability and the required mechanical properties of the alloys should provide the aluminum matrix composition;

– the morphology of the eutectic phase should be compact immediately during crystallization or after annealing like the silicon phase particles in the Al — Si based alloys;

– the crystallization range (especially effective) should be as narrow as possible.

So the six-component system Al – Zn – Mg – Cu – Fe – Ni – (Si) was chosen as base of the new high-strength sparingly alloyed cast aluminum alloys. This system was chosen for the following reasons:

1. Zinc, magnesium and copper are the main alloying elements. These elements promote hardening due to formation of secondary segregations of various metastable phases upon aging. For this reason, their total content in the aluminum solid solution (Al) before aging should be maximum.

2. Nickel and iron are the new eutectic-forming components. In this case, the iron becomes an alloying element, rather than a harmful impurity.

3. Silicon is an inevitable impurity.

The distribution of these elements in the phases of crystallization origin and secondary segregations in the Al – Zn – Mg – Cu – Fe – Si – Ni system is presented in Table 2.

Earlier studies of alloys based on the Al – Zn – Mg – Ni system [13–14] showed that a high level of the mechanical properties can be reached at zinc and magnesium content of 6–8 and 2–4%, respectively. These ranges are the basis for the strongest aluminum alloys. The same ranges are considered as promising compositions for the development of sparingly alloyed high-strength nikalins based on the (Al) + Al_9FeNi eutectic.

According to the data [1, 18] nickel and iron do not form phases with magnesium and zinc. This means that the phase composition of the Al – Zn – Mg – Ni – Fe system can be analyzed from two ternary diagrams: Al – Zn – Mg (the aluminum matrix) and Al – Ni – Fe

Table 2.

Distribution of alloying elements and impurities in the phases of alloys of the Al – Zn – Mg – Cu – Fe – Si – Ni system [1, 3, 17, 18]

Phases	Zn	Mg	Cu	Fe	Si	Ni
Secondary segregations						
T (Al_2Zn_3Mg)	+	+	+	–	–	–
M ($MgZn_2$)	+	+	+	–	–	–
S (Al_2CuMg)	–	+	+	–	–	–
Al_2Cu	–	–	+	–	–	–
Phases of crystallization origin						
Al_3Fe	–	–	–	+	–	–
Al_8Fe_2Si	–	–	–	+	+	–
Al_7Cu_2Fe	–	–	+	+	–	–
Al_9FeNi	–	–	–	+	–	+
Al_3Ni	–	–	–	–	–	+
$Al_3(Ni, Cu)_2$	–	–	+	–	–	+
Al_7Cu_4Ni	–	–	+	–	–	+
Mg_2Si	–	+	–	–	+	–
T	+	+	+	–	–	–
M	+	+	+	–	–	–
S	–	+	+	–	–	–
Al_2Cu	–	–	+	–	–	–

(inclusions of Ni- and Fe-containing phases of crystallization origin). However, it should be noted that studies aimed at plotting fragments of the Al – Zn – Mg – Cu diagram have been performed as early as the 1960–1970s [17, 18]. Little was added in subsequent years though the data were obviously insufficient for developing alloys of a new generation.

In order to analyze the cooperative effect of zinc and magnesium on the phase composition of aluminum matrix at potential temperatures of aging, the isothermal sections (Fig. 1) of the Al – Zn – Mg – Cu system at 125 °C and 250 °C were calculated using Termo-Calc software.

Fig. 1 shows that the (Al) solid solution in the temperature range of 125–250 °C can be in equilibrium with the $MgZn_2$ (*M*) and $Al_2Mg_3Zn_3$ (*T*) phases, which form the phase regions (Al) + *M*, (Al) + *M* + *T*, and (Al) + *T*. The two phase regions (Al) + *M* + *T* and (Al) + *T* correspond to the considered range of zinc (6–8)% and magnesium (2–4)% content under study.

In order to optimize the chemical composition of the new alloys the thermodynamic calculations of the Al – Zn – Mg – Cu – Fe – Ni multicomponent phase diagram were produced by Termo-Calc. The results of thermodynamic calculations have shown that the addition of copper to Al – Zn – Mg – Cu based alloys containing iron and nickel is more harmful rather than useful. According to the isothermal section (Fig. 2, *a*), the content of copper-bearing phases, i. e., Al_7Cu_2Fe, Al_7Cu_4Ni, Al_9FeNi, $Al_3(Ni, Cu)_2$, $S(Al_2CuMg)$ is the highest and some of these phases may be present in the final structure. Most of these phases form during solidification (primarily by eutectic reactions) and have an acicular morphology and affect negatively the mechanical properties. However, if limited to a copper concentration up to about 1% (wt.) (Fig. 2, *b*), the number of excess phases decreases substantially (Al_3Ni, Al_9FeNi, Al_3Fe). This facilitates a search for the alloy compositions for which the desired structure (aluminum solid solution with Al_9FeNi phase inclusions) can be formed.

The concentrations of nickel and iron corresponding phase region (Al) + Al_9FeNi, marked in Fig. 2, *b*, are optimal for the creation of sparingly alloyed high-strength nikalins, for the following reason: the development of sparingly alloyed alloy, the nickel content is assumed to be minimum, whereas the iron content is maximum. This condition corresponds to the phase boundary (Al) + Al_9FeNi/(Al) + Al_9FeNi + Al_3Fe. Since the appearance of the needle-shaped Al_3Fe phase is undesirable, this boundary should be considered as the maximum allowable iron and nickel content.

In order to analyse the impact of nickel and iron on the phase composition of new alloys during equilibrium solidification, the liquidus surface and the polythermal

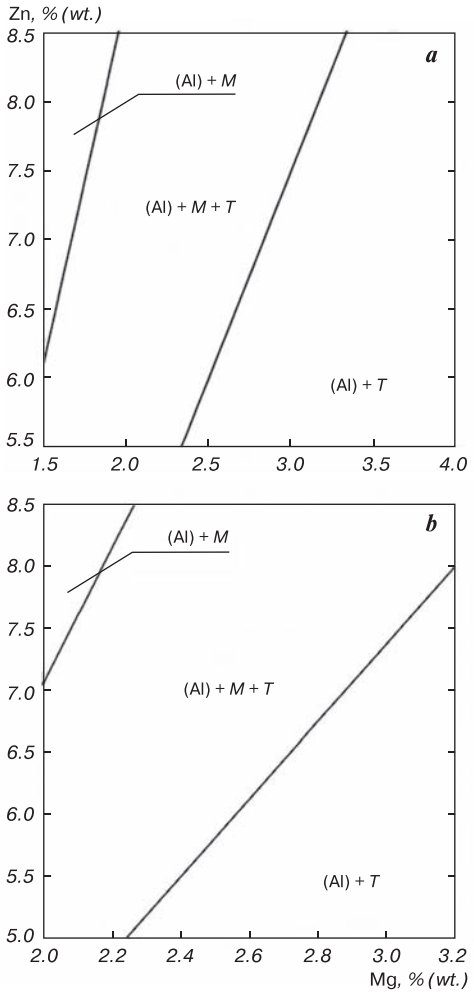

Fig. 1. Isothermal sections for the Al – Zn – Mg – Cu system at: *a* — 0.2% Cu and 125 °C; *b* — 0.2% Cu and 250 °C

section of the Al – Zn – Mg – Cu – Fe – Ni system at constant concentrations of zinc and magnesium were obtained by Thermo-Calc (Fig. 3). Since the primary crystals of any Fe- and Ni-primary phase are undesirable, the boundaries of primary crystallization of different phases (the liquidus projection) were computed. Fig. 3, *a* shows that the nickel concentration increase leads to a decrease of the allowable iron concentration, which follows more visually from the polythermal sections (Fig. 3, *b*). According to the polythermal section, the appearance of primary needle-shaped plates of the Al_3Fe phase at a Ni content of 1% (wt.) is expected beginning from ~0.7% (wt.) of Fe (Fig. 3, *b*). The decrease of the iron concentration up to about 0.2% of Fe does not change the phase composition and has a low effect on the liquidus and solidus temperatures. The optimal concentrations region of nickel and iron are marked in Fig. 3, *a*.

The following conclusions were made on the basis of the above analysis of the main conclusions to optimize the composition of new sparingly alloyed high-strength aluminum alloys based on the Al – Zn – Mg – (Cu) – Ni – Fe system:

1. From the standpoint of economic efficiency the concentration of nickel should be the lowest and that of iron should be the highest. This requirement is met at the phase boundary (Al) + Al_9FeNi/(Al) + Al_9FeNi + + Al_3Fe. However, since the Al_3Fe phase, which has an acicular form, is undesirable, we should provide a somewhat higher proportion of Ni to Fe.

2. In order to obtain maximum content of eutectic inclusions of Al_9FeNi we should orient at the boundary of primary crystallization of (Al). At best, crystallization should start with a reaction $L \rightarrow$ (Al) + Al_9FeNi. In that case the casting properties of the alloy will be the highest.

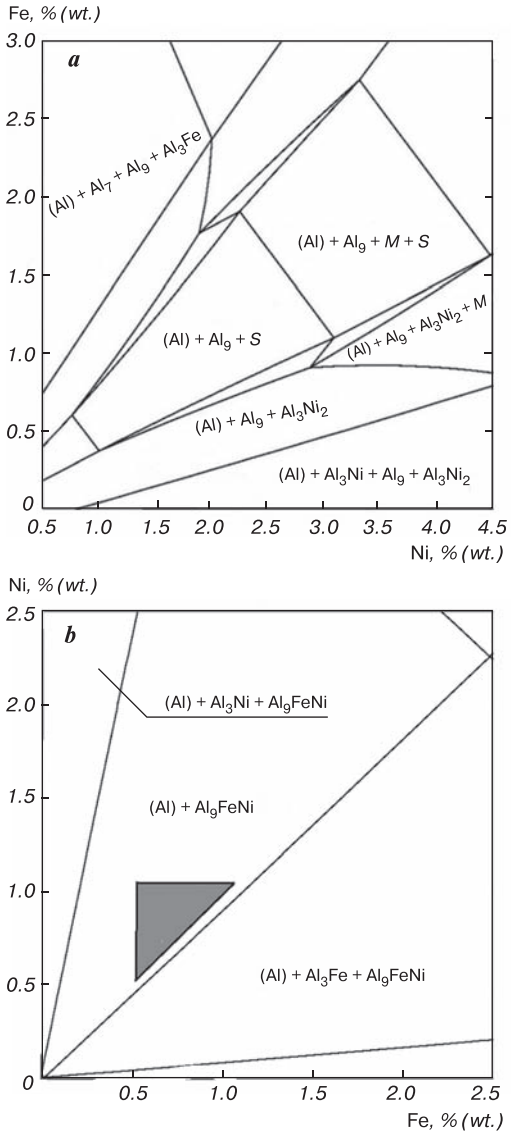

Fig. 2. Isothermal sections for the Al – Zn – Mg – Cu – Ni – Fe system at:
a — 8% Zn, 2% Mg, 2% Cu and 460 °C; *b* — 6.3% Zn, 2.1% Mg, 0.15% Cu and 570 °C

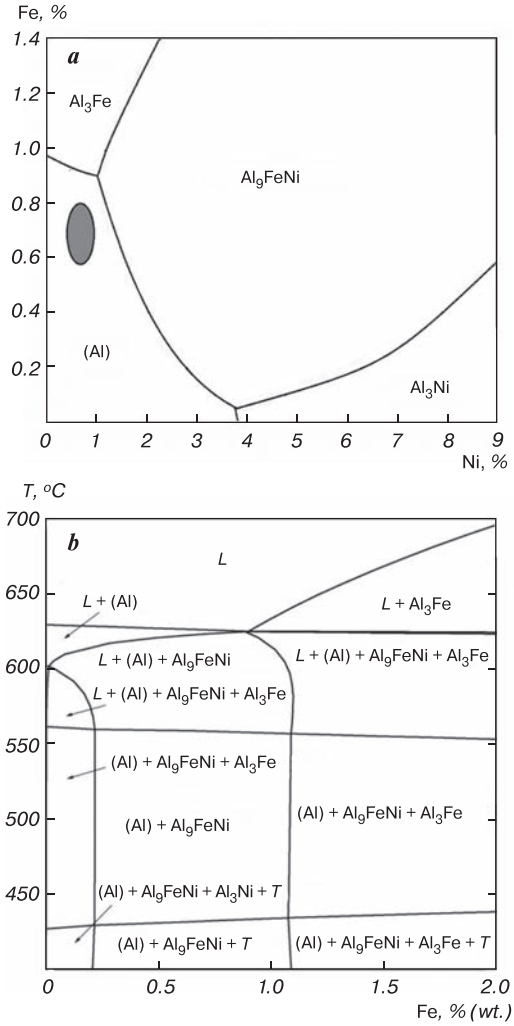

Fig. 3. Liquidus projection in the Al – Zn – Mg – Fe – Ni system at 7% Zn and 3% Mg (*a*) and polythermal section for the Al – Zn – Mg – Fe – Ni system at 7% Zn, 3% Mg and 1% Ni (*b*)

3. In order to prevent crystallization of a large number of harmful precipitates ($Al_6(Fe, Cu)$, Al_7Cu_2Fe, Al_7Cu_4Ni, $Al_3(Ni, Cu)$, $S(Al_2CuMg)$, Al_2Cu) copper content should not exceed 1% (wt.).

Based on these findings, we have selected the following ranges of concentrations of (0.5–1.0)% Ni and (0.4–0.8)% Fe, satisfying the conditions described above. For further experimental studies, the most sparingly alloyed alloy ATs6N0.5Zh (Al – 6.3% Zn – 2.1% Mg – 0.2% Cu – 0.4% Fe – 0.6% Ni) was selected.

In accordance with Fig. 4, *a* equilibrium solidification of the model alloy ATs6N0.5Zh begins with the allocation of aluminum solid solution (Al) primary crystals. Thereafter, the double eutectic reaction L (Al) + Al_9FeNi occurs. Equilibrium crystallization ends in two-phase region (Al) + Al_9FeNi.

The results of the solidification presented above were calculated in equilibrium conditions. Using the Sheil model it's possible to calculate temperatures of liquidus and non-equilibrium solidus in conditions close to the real non-equilibrium solidification (Fig. 4, *b*). This is a model of the dependence of the solid phases fracture on temperature in the interval of the non-equilibrium solidification. According to the Sheil model after the binary eutectic reaction L (Al) + Al_9FeNi the new ternary eutectic reaction L (Al) + Al_9FeNi + T proceeds. This leads to the appearance of a new non-equilibrium phase (T) and a significant reduction of the solidus.

Calculated data obtained from the Sheil model agree well with the experimental data. On the experimental cooling curve (Fig. 4, *c*) the inflection points corresponding to the three transformations ($L \rightarrow$ (Al) (T_L), L (Al) + Al_9FeNi (T_e) and L (Al) + Al_9FeNi + T (T_{ns})) were detected. The analysis results of the as-cast ATs6N0.5Zh alloy structure also confirm the calculated and experimental data. The Al_9FeNi phase and non-equilibrium T phase particles from the degenerate eutectics (Al) + Al_9FeNi and (Al) + Al_9FeNi + T are in equilibrium with the (Al) solid solution.

Based on the data presented above the two-stage homogenization annealing regimes were selected as the following: $t_1 = (t_{ns} - 10)$ and $t_2 = (t_s - 10)$, where t_{ns} and t_s (°C) are the temperatures of the non-equilibrium and equilibrium solidus lines, respectively.

The first stage of homogenizing annealing (at t_1 ~ ~ 450 °C) is intended for dissolution of the nonequilibrium T phase particles. However, the skeleton-like morphology of Al_9FeNi particles changes slightly even after 10-h holding at 450 °C. This is related to the low diffusion activity of iron and nickel atoms. Therefore,

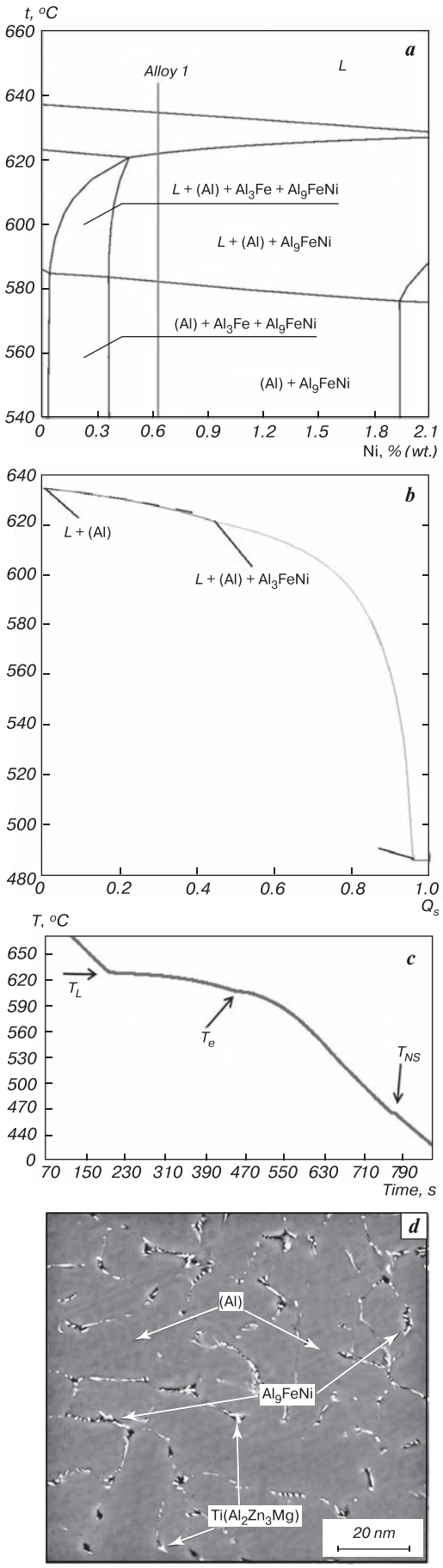

Fig. 4. Polythermal section for the Al – Zn – Mg – Fe – Ni system at 6.3% Zn, 2.1% Mg, 0.2% Cu and 0.4% Fe (*a*); dependences of the solid phases fracture from the temperature in the interval of the non-equilibrium solidification of the ATs6N0.5Zh alloy (*b*); the cooling curve of the ATs6N0.5Zh alloy (*c*); as-cast structure of ATs6N0.5Zh alloy (*LM*) (*d*)

to obtain relatively globular Al_9FeNi-phase inclusions, the second stage of heat treatment at temperatures above 500 °C was used.

To estimate the possibilities of a practical application of the thermodynamic calculations results, the structure of the model alloy based on the Al – Zn – Mg – (Cu) – Ni – Fe system after homogenizing annealing at 450 °C for 3 h was analyzed using electron microscopy and EPMA (Fig. 5).

The EPMA data allowed to determine that the ternary (AlFeNi) phase is in equilibrium with the (Al) solid solution in the alloy structure. In accordance with the literature data and the results of thermodynamic calculations, this phase is Al_9FeNi phase inclusions from the degenerate eutectic (Al) + Al_9FeNi. Thus, as it was predicted by the thermodynamic calculations, the structure of the model alloy after homogenizing annealing contains (Al) primary crystals and Al_9FeNi phase inclusions from the degenerate eutectic. Note that the possibility of predicting phase composition and structure of the alloys for the multicomponent system under study solves the problem of minimizing the number of experimental studies and allows one to find the optimum compositions of alloying elements to achieve the required level of properties.

The use of alloy ATs6N0.5Zh makes it possible to obtain high mechanical properties in different castings. After an appropriate heat treatment (quenching and the following two-step artificial aging), the new alloy has the following properties: $\sigma_r > 500$ MPa, $\sigma_{0.2} > 450$ MPa, $\delta > 6\%$. Such a quite favorable combination of strength and ductility is a result of uniform distribution of Al_9FeNi inclusions and their relatively compact morphology (Fig. 5, *a*). This promotes uniform plastic straining in the process of loading, which is confirmed by the results of fracture surface analyses (Fig. 6). The figure shows the structure of fracture surfaces of the ATs6N0.5Zh alloy after artificial aging. The fracture surfaces contains numerous dimples with a size of 20–30 μm that bear inclusions of an Al_9FeNi phase inside. Traces of intergrain fracture typical for high-alloyed alloys without eutectic inclusions are not observed. This is connected with the fact that

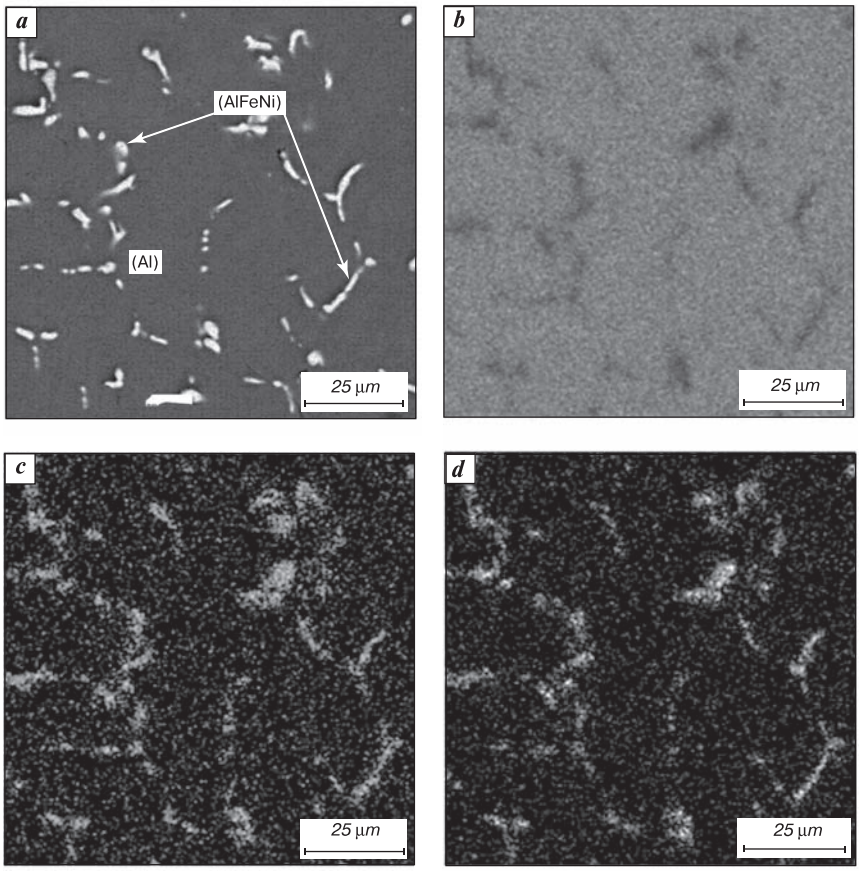

Fig. 5. Structure of ATs6N0.5Zh alloy after homogenizing annealing (SEM) (*a*); map of Al (*b*) Fe (*c*) and Ni (*d*) distribution

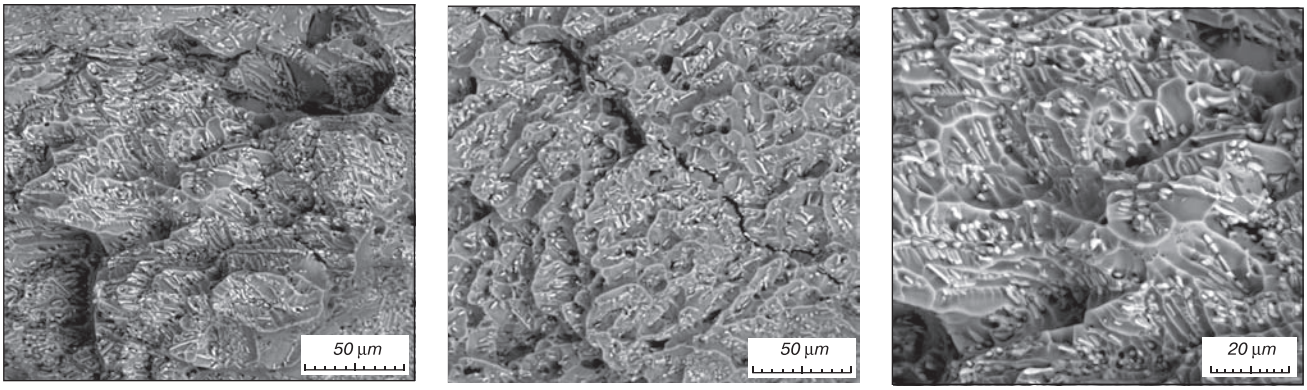

Fig. 6. Fracture surfaces of ATs6N0.5Zh alloy at different magnifications (SEM)

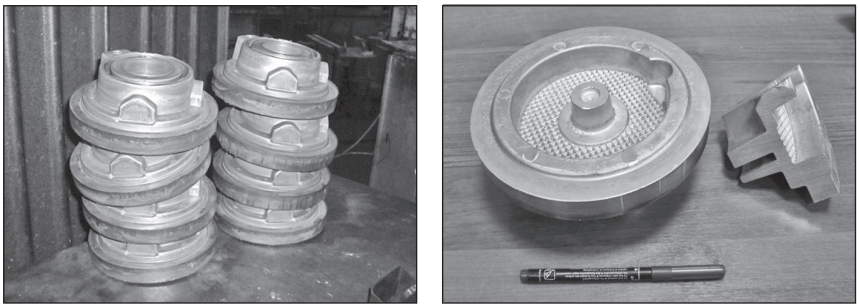

Fig. 7. Alloy ATs6N0.5Zh casting

the interphase boundaries (Al)/Al_9FeNi as high angle boundaries are effective places to drain vacancies. As a result the supersaturated solid solution (Al) decomposition occurs more uniformly and completely without the grain boundary precipitates which are characteristic for the base alloy without nickel and iron.

Nikalin ATs6N0.5Zh has proved to be suitable for making shapes cast into metallic molds by various methods. In particular, castings obtained by liquid forging (Fig. 7, *a*, *b*) have σ_r ~ 500 MPa, $\sigma_{0.2}$ ~ 450 MPa, δ ~ 4.7%. The ATS6N0.5ZH alloy has shown high technology for the preparation of shaped castings by crystallization under pressure. At external survey no found hot cracks or shrinkage cavities. The observed geometry of the sample is correct.

Conclusions

1. *Thermodynamic calculations of the phase composition of the* Al – Zn – Mg – (Cu) – Fe – Ni *multicomponent system as applied to an experimental high-strength aluminum alloys based on an* (Al) + Al_9FeNi *eutectic were performed by Thermo-Calc software. Reducing the copper content up to 1% leads to a significant simplification of the alloy phase composition. There are only three phases* (Al_3Ni, Al_9FeNi, Al_3Fe) *which are in equilibrium with the aluminum solid solution at the temperature above the solvus.*

2. *The phase boundary* (Al) + Al_9FeNi/(Al) + Al_9FeNi + + Al_3Fe *is the most suitable for the structure of the new sparingly alloyed high-strength alloy based on the* Al – Zn – Mg – Cu –Fe – Ni – Si *system. Since the appearance of the iron-bearing phases is unacceptable, the boundary of coarse primary crystals formation of* Al_3Fe, Al_9FeNi, Al_3Ni *phases depending on the concentration of iron and nickel was determined. The results show that the nickel concentration increase leads to a decrease in the allowable concentration of iron. Specifically, the appearance of primary* Al_3Fe *intermetallic plates at a nickel content up to 1% (wt.) should be expected beginning from an iron content of ~0.7% (wt.).*

3. Based on the calculated and experimental data the chemical composition of the model alloy was selected. Experimental studies have shown that the structure of the model alloy after homogenizing annealing contains (Al) *primary crystals and* Al_9FeNi p*hase inclusions from the degenerate eutectic as predicted by thermodynamic calculation.*

4. Uniform distribution of Al_9FeNi *inclusions in* (Al) *and their relatively compact morphology provide a high set of strength and ductility of the new alloy. As the results of the fracture surface analysis of samples after artificial ageing, the* Al_9FeNi *phase particles prevent the formation of grain boundary precipitates of reinforcing metastable phases, so the fracture character of loaded samples changes from brittle intergranular to more ductile dimple fracture.*

5. Using the model alloy the quality products were obtained by liquid forging and argon-arc welding. The new material possesses an enhanced combination of mechanical (σ_r ~ 500 MPa, $\sigma_{0.2}$ ~ 450 MPa, δ ~ 4.7%) *and casting properties and material-saving. It can be recommended to replace conventional industrial alloys of AA7050 type.*

Research sponsored by the Ministry of Education and Science of the Russian Federation (Agreement 14.578.21.0039 (RFMEFI57814X0039)) in the framework of the Federal Target Program "Researches and developments on priority directions of scientific-technological complex of Russia for 2014–2020" and the grant of the Russian Federation President for Support of the Leading scientific schools, НШ-9899.2016.8.

References

1. Polmear I. J. Light Metals: From Traditional Alloys to Nanocrystals. Oxford : Elsevier/Butterworth-Heinemann, 2006. 421 p.

2. Li Jin-feng, Peng Zhuo-wei, Li Chao-xing et al. Mechanical properties, corrosion behaviors and microstructure of 7075 aluminum alloy with various aging treatments. Transactions of Nonferrous Metals Society of China. 2008. Vol. 18. pp. 755–762.

3. Ibrahim M. F., Samuel A. M., Samuel F. H. A preliminary study on optimizing the heattreatment of high strength Al –Cu – Mg – Zn alloys. Materials and Design. 2014. Vol. 57. pp. 342–350.

4. Wenchao Yang, Shouxun Ji, Mingpu Wang, Zhou Li. Precipitation behaviour of Al – Zn – Mg – Cu alloy and diffraction analysis from g0 precipitates in four variants. Journal of Alloys and Compounds. 2014. Vol. 610. pp. 623–629.

5. Adrien J., Maire E., Estevez R., Ehrstrom J. C., Warner T. Influence of the thermomechanical treatment on the microplastic behaviour of a wrought Al – Zn – Mg – Cu alloy. Acta Materialia. 2004. Vol. 52. p. 1653–1661. doi: 10.1016/j.actamat.2003.12.009

6. Xu Fang, Min Song, Kai Li, Yong Du, Dongdong Zhao, Chao Jiang, Hong Zhang. Effects of Cu and Al on the crystal structure and composition of η ($MgZn_2$) phase in over-aged Al – Zn – Mg – Cu alloys. Journal of Materials Science & Technology. 2012. Vol. 47. pp. 5419–5427.

7. Myriam N., Alexis D. Characterisation and modelling of precipitate evolution in an Al – Zn – Mg alloy during non-

isothermal heat treatments. Acta Materialia. 2003. Vol. 51. pp. 6077–6094.

8. Xu Fang, Yong Du, Min Song, Kai Li, Chao Jiang. Effects of Cu content on the precipitation process of Al – Zn – Mg alloys. Journal of Materials Science & Technology. 2012. Vol. 47. pp. 8174–8187.

9. Marlaud T., Deschamps A., Bley F., Lefebvre W., Baroux B. Evolution of precipitate microstructures during the retrogression and re-ageing heat treatment of an Al – Zn – Mg – Cu alloy. Acta Materialia. 2010. Vol. 58. pp. 4814–4826. doi: 10.1016/j.actamat.2010.05.017

10. Zolotorevskiy V. S., Belov N. A. *Metallovedenie liteynykh aluminievykh splavov* (Materials Science of Casting Aluminum Alloys). Moscow : MISiS, 2005. 376 p.

11. Zolotorevskiy V. S., Belov N. A. Materials Science of Casting Aluminum Alloys. MISiS : Moscow, 2005. 376 p.

12. Belov N. A., Zolotorevskiy V. S. Liteynye splavy na osnove aluminievo-nikelevoy evtektiki (nikaliny) kak vozmozhnaya alternativa siluminam (Casting alloys based on aluminum–nickel eutectic (nikalins) as a possible alternative for silumins). T*svetnye Metally = Non-ferrous metals*. 2003. No. 2. pp. 99–105.

13. Belov N. A., Zolotorevskiy V. S. The effect of nickel on the structure, mechanical and casting properties of 7075 aluminum alloy. Materials Science Forum. 2002. 396–402.

14. Pat. 2245383 RF. Aluminum-base material/ Belov N. A. et al. *Byull. Izobr. Polezn. Modeli*, 2005. No. 3.

15. Belov N. A., Tagiev E. E. Eutectic structures in alloys based on solid solution of the Al – Zn – Mg – Cu system. Izv. Vysh. Ucheb. Zaved., Tsvetn. Met. 1991. Vol. 2. pp. 95–98.

16. Lijun Zhang, Jiong Wang, Yong Du, Rongxiang Hu, Philip Nash, Xiao-Gang Lu and Chao Jiang. Thermodynamic properties of the Al – Fe – Ni system acquired via a hybrid approach combining calorimetry, first-principles and CALPHAD. Acta Materialia. 2009. Vol. 57. pp. 5324–5341. doi: 10.1016/j.actamat.2009.07.031

17. Mondolfo L. F. *Structura I svoystva aluminievykh splavov* (Structure and Properties of Aluminum Alloys). Moscow : Metallurgiya, 1979. 640 p.

18. Zakharov M. *Promyshlennye splavy tsvetnykh metallov* (Commercial alloys of non-ferrous metals). Moscow : Metallurgiya, 1980. 256 p.

NFM

Modeling of butt and lap joint laser welding of aluminum alloys and constructional steel sheets

UDK 621.791.725

A. N. Shlegel, *Head of Laboratory of the laser technologies research and application of the Engineering Center, Assistant Professor of Automation of technological processes Department* [1], *e-mail: shlegel81@rambler.ru*
N. N. Evtikheev, *Head of Laser Physics Department*[2]
D. S. Gusev, *Engineer of Laboratory of the laser technologies research and application of the Engineering Center*[1]
A. B. Ivanchenko, *Assistant Professor, Mechanical Engineering Department*[1]

[1] *Vladimir State University named after Alexander and Nikolay Stoletovs, Vladimir, Russia.*
[2] *National Research Nuclear University MEPhI (Moscow Engineering Physics Institute), Moscow, Russia.*

Recently the most claimed at the market are technologies of body components and parts obtaining which combine multi-metal welding. Such technologies are especially needed on the railway and motor transport as well as in special production. Manufacturing of the motor transport frame units consisting of steel skeleton and sheet aluminum coating allows to improve their corrosion resistance and essentially decrease weight of the carriers, which consequently contribute to the fuel consumption lowering. Residual deformations originated from the welding process negatively affect the welded construction qualitative characteristics, such as strength, harshness, containment, corrosion resistance, etc. Stress level reduction is available by means of the welded seam form and quality, which depend on the welding process technological parameters. Determination of rational technological parameters of the welding processes requires taking into account the used rolled metal features, namely different thermal conduction of materials, significantly bigger (≈50%) coefficient of linear (thermal) expansion inherent to non-ferrous metals as compared to carbon steel, foamed metal-oxide layer formation on the surface of the weld leading to deterioration of corrosion resistance.
The article is devoted to the modeling process of the laser welding modes impact upon strength properties of the weld of aluminum alloy and constructional steel sheets. Presented are an algorithm and results of the finite-element analysis simulation modeling of the butt and lap joint laser welding by the example of AMg2M (АМг2М) aluminum alloy and St3 (Ст3) steel samples. Weld strength properties obtained experimentally and by modelling are compared. It is demonstrated that the worked out simulation model of multi-metal sheets laser welding may be used for theoretical study of the butt and lap joint welding of any other heterogeneous materials.

Key words: laser welding, lap joint welding, butt welding, simulation model, method of finite-element analysis, aluminum alloy, steel, residual stresses, ultimate breaking load, tensile strength.

DOI: *http://dx.doi.org/10.17580/nfm.2016.01.05*